Bedingungen ist das Verhältnis der Ionen der Masse 313 und 314 (100:40), bei Aufnahme mit einem Varian CH4-Gerät (Direkteinlaß, 70 eV, Verdampf.-Temp. 125 °C, Ionenquelle 50 °C) gerade umgekehrt. Bei DANS-CBN betrifft dies insbesondere das Verhältnis der Ionen 309 und 310. Möglicherweise erfolgt im CH4-Massenspektrometer teilweise Zersetzung oder es findet eine Umlagerung statt. Ähnliche Effekte zeigen Spektren von Egge *et al.* [8].
In der Regel ist (abhängig von der Menge und dem Gehalt des gerauchten Haschisch) eine Stunde nach dem Rauchen noch genügend THC im Speichel, um ein Massenspektrum des Dansyl-Derivates zu erhalten und somit eindeutig den Abusus von Haschisch zu beweisen. Fluorometrisch war THC in nahezu allen Speichelproben auch 6 h nach dem Rauchen zu erkennen. Längere Zeiten wurden bisher nicht geprüft.

Die Arbeit der Göttinger Gruppe wurde mit Hilfe von Forschungsmitteln des Landes Niedersachsen gefördert.

Eingegangen am 18. Januar 1973

[1] Just, W. W., Werner, G., Wiechmann, M.: Naturwissenschaften **59**, 222 (1972). — [2] Lemberger, L., et al.: Science **173**, 72 (1971); Lemberger, L., et al.: ibid. **170**, 1320 (1970); Lemberger, L., Axelrod, J., Kopin, I. J.: Pharmacol. Rev. **23**, 371 (1971). — [3] Skinner, R. F.: Proc. West. Pharmacol. Soc. **15**, 136 (1972). — [4] Christiansen, J., Rafaelsen, O. J.: Psychopharmakologia (Berl.) **15**, 60 (1969). — [5] Spiteller, G., Kaschnitz, R.: Mh. Chem. **94**, 964 (1963); Grostic, H. F., Wnuk, R. J., Mackellar, F. K.: J. Amer. chem. Soc. **88**, 4664 (1966). — [6] Budzikiewicz, H., et al.: Tetrahedron **21**, 1881 (1965). — [7] Egge, H., et al.: Z. Naturforsch. **26b**, 229 (1971); Creveling, C. R., Kondo, K., Daly, J. W.: Clin. Chem. **14**, 302 (1968). — [8] Seiler, N., Schneider, H., Sonnenberg, K.-D.: Z. Anal. Chem. **252**, 127 (1970).

Visualization by Freeze-Facturing of Regular Structures in Glial Cell Membranes

R. Dermietzel

Institut für Topographische Anatomie,
Universitätsklinikum der Gesamthochschule Essen

Gap junctions or nexuses have been described in cell membranes of vertebrates and invertebrates [1, 2]. There are several reasons to believe that they represent the locus for the direct exchange of ions [3] mediating the electric coupling from cell to cell. In a recent freeze-fracturing study Staehelin [4] demonstrated various gap junctions in intestinal epithelial cell membranes, which he categorized as types I, II and III, according to the size and specific arrangement of the particles.
We report here gap junctions visualized by freeze-fracturing in astrocytic membranes from the periventricular region of the 4th ventricle of cats. The membrane faces in freeze-fractured replicas usually contain particles scattered over the whole membrane; at gap junctions they are arranged as in a honeycomb. We found many such structures in our material in various extensions (Fig. 1a). Particle size (8 nm) and center-to-center spaces (9 ± 0.4 nm) are in accordance with the results obtained in other tissues. Besides this type of gap junction (type I according to Staehelin [4]), another type of particle aggregation was seen, consisting of small rectangular arrays of particles or pits. These were found either in close relation to type-I gap junctions or distributed at random over the membranes of the astrocytes. In contrast to the particles of type III [4], these particles had a median diameter of 9–10 nm and seemed flatter than the particles of the type-I nexus; they were also much closer together so that hardly any interspace could be detected.
The most striking finding, however, was that the rectangular arrays of particles could be observed in various stages of aggregation and extension, from single rows to planes where the arrangement is composed of several linear arrays of particles. These different types of packing were frequently seen in both the A and B faces (Fig. 1b).
These findings further support the concept of a dynamic membrane and the working hypothesis of the dynamic character of the connections which are involved in cell-to-cell communication. Contrary to the interpretation of Staehelin [4], our observations strongly suggest that the rectangular particle aggregations found in glial cell membranes do not represent a special type of gap junction so much as subunits of functional nexuses in different stages of integration and disintegration.

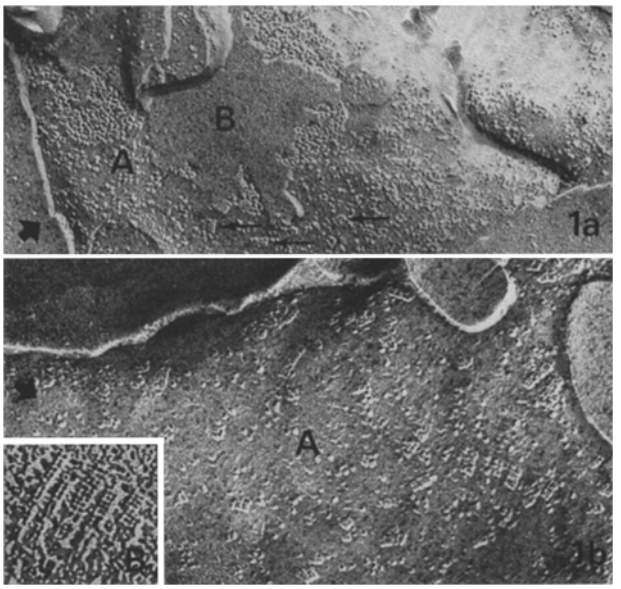

Fig. 1. a) Gap junction in an astrocytic membrane. The A face displays particles and the B face pits. Arrows indicate small rectangular "subunits"; 62000:1. b) A face showing rectangular aggregates at various stages. The particles of the "subunits" seem to be composed of at least four smaller particulate elements; 93000:1. Inset: B face of particles lying in a rectangular array consisting of several parallel rows; 105000:1

Supported by the "Sonderforschungsbereich" Bionach 114.

Received January 25, 1973

[1] Revel, J. P., Karnovsky, M. J.: J. Cell Biol. **33**, C 7 (1967). — [2] Gilula, N. B., Satir, P.: ibid. **51**, 869 (1971). — [3] Loewenstein, W. R., Nakas, M., Socolar, S. F.: J. Gen. Physiol. **50**, 1865 (1967). — [4] Staehelin, L. A.: Proc. Nat. Acad. Sci. **69**, 1318 (1972).

Postnatal Development of Myelinated Fibers in the Rat Trigeminal Nerve

K. Mira* and W. Wechsler

Max-Planck-Institut für Hirnforschung, Köln

Quantitative studies of the development of the trigeminal nerve are lacking. We initiated such a study in rats both to supplement earlier comparative anatomical observations of the trigeminal nerves of dog and man [1], and because such studies are needed as a solid basis for the evaluation of early or late nerve fiber changes produced under a variety of pathological conditions.
Morphometric studies were made of the normal sensory root of the trigeminal nerve of BD-IX rats [2] in order to determine size distribution profiles for myelinated nerve fibers at particular stages of postnatal development. The size distribution of the myelinated nerve fibers was measured after the first week of life, although myelination is already evident in some nerve fibers at birth. The diameter of these fibers was determined by light microscopy using the ocular grid micrometer with the oil immersion objective lens (magnification 800 ×) and on microphotos (magnification 1600 ×) of areas representing the mandibular, maxillary and ophthalmic branches of this cranial nerve.
From various age groups (see Table 1) five trigeminal nerves were prepared for electron microscopy (fixation with phosphate-buffered 3% glutaraldehyde and 2% osmiumtetroxide and embedding in araldite). Cross sections 1 µm thick near the pons ($S1$) or the trigeminal ganglion ($S2$) were stained with toluidine blue.
Our results are summarized in Table 1. During the first month of postnatal development the distal part of the sensory root ($S2$) apparently contains more myelinated nerve fibers under

